Journal of Applied Polymer Science

Flow Improvement of Liaohe Extraheavy Oil with Comb-Type Copolymers

Hejian Jiang,[1] Jun Xu,[1] Xiaoming Wei,[2] Tongshuai Wang,[1] Weina Wang,[1] Li Li,[1] Xuhong Guo[1]

[1]State Key Laboratory of Chemical Engineering, East China University of Science and Technology, Shanghai 200237, China

[2]Petrochina Liaohe Oilfield Company, Panjin 124010, China

Correspondence to: J. Xu (E-mail: xujun@ecust.edu.cn) or X. Guo (E-mail: guoxuhong@ecust.edu.cn)

ABSTRACT: Liaohe extraheavy oil is a kind of special crude oil with high paraffin and asphaltene contents and a pour point of up to 60°C. To improve its flowability, comb-type poly(maleic alkylamide-*co*-α-octadecene) copolymers (MACs) with various amidation ratios were synthesized and used. Model oils containing paraffin mixtures with the same average carbon number to Liaohe extraheavy oil with and without asphaltene were prepared to explore the effect of the MACs on paraffin crystallization and asphaltene dispersion, respectively. We found that MACs reduced the yield stress, changed the size and shape of the paraffin crystals, and obstructed the paraffin crystallization for both model oils and extraheavy Liaohe oils as observed by rheology, polarizing light microscopy, X-ray diffraction, and differential scanning calorimetry. The MACs seemed to be an ideal candidate for improving the flowability of Liaohe extraheavy oils. © 2013 Wiley Periodicals, Inc. J. Appl. Polym. Sci. **2014**, *131*, 40082.

KEYWORDS: applications; functionalization of polymers; oil and gas; rheology

Received 30 August 2013; accepted 19 October 2013

DOI: 10.1002/app.40082

INTRODUCTION

Crude oil is a complex hydrocarbon mixture mainly consisting of paraffins, aromatics, resins, and asphaltenes.[1] Wax crystallization presents a serious challenge in the production, transportation, and refinement of crude oil. Above the wax apparent temperature (WAT), crude oil usually behaves as a Newtonian fluid with a low viscosity.[2] Nevertheless, below the WAT, the solubility of long-chain paraffins and asphaltenes in light hydrocarbon drops, and the paraffins generally crystallize as an interlocking network and thereby form three-dimensional structures. When the temperature approaches the pour point, the lowest temperature at which oil can flow, the deposited paraffin crystals and aggregated asphaltenes reduce the flowability of crude oil and even block the pipeline.[3–8] The flowability of waxy crude oil, which includes many rheological properties, such as yield stress (τ_y), viscosity, pour point, and WAT, is sensitive to changes in the temperature. Flow assurance has become a major technical and economic hurdle in the transportation of crude oil in cold environments, such as in northern China in the winter or in deep-sea pipelines. To solve those problems, thermal, mechanical, and chemical methods are available. Among the previous methods, chemical methods by the feeding of polymer additives into crude oil have often been used with success.[9]

Polymers with crystalline/amorphous diblock structures play an important role in the improvement of the flowability of crude oil as wax inhibitors; examples of wax inhibitors include ethylene–vinyl acetate copolymer,[10,11] poly(ethylene–propylene),[12] poly(ethylene–butene),[13–15] and comb-type poly(maleic anhydride-*co*-olefin)s esterified by alkyl alcohols.[16] Typically, among these polymers, they all have nonpolar branches and/or polar parts. These copolymers can interfere in the wax crystal growth and prevent the asphaltenes from aggregating and forming interlocking networks. The synthesis of more effective polymer additives has been a research hotspot in this area.[17–19]

Liaohe extraheavy oils are special crude oils stored in the Liaohe oilfield located in north China with an extremely high content of paraffins and asphaltenes. These oils appear to be solid at room temperature and cannot flow without heating. Their recovery and transportation by oil pipes are extremely difficult and expensive.

In our previous work, we synthesized poly(maleic acid alkylamide-*co*-α-octadecene) copolymers (MACs).[20–22] They significantly improved the flowability of model waxy oils and crude oils from the Halliburton and Tomark Industries.[22–24] It has been found that the efficiency of MACs as a flow improver mainly depends on the composition of the oils and the polar/nonpolar group ratio of the polymer additives. The distribution of the long-chain paraffins and the amount of asphaltenes in crude oils strongly affect their rheological behaviors.[13,25,26] Also, the chemical structure of comb-type copolymers is directly

Table I. Compositions and Physical Properties of CO-1 and CO-2

Crude oil	Paraffin content (%)	Asphaltene content (%)	Density at 20°C (g/cm^3)	Pour point (°C)	Viscosity at 70°C (mPa s)
CO-1	38.5	15.6	0.8676	54	7.2
CO-2	35.5	13.1	0.8557	60	8.1

associated with their performance in the improvement of oil flowability.

In this study, MACs with various ratios of nonpolar to polar groups were synthesized. To mimic extraheavy Liaohe oils, two kinds of model oils with the same average carbon number of paraffins with and without asphaltenes were prepared. A rheological method, differential scanning calorimetry (DSC), polarized light microscopy (PLM), and X-ray diffraction (XRD) were used to characterize the effect of the MACs on the paraffin crystallization and flowability of model oils and Liaohe extraheavy crude oils. A mechanism of how the comb-type MACs improved the flowability of the Liaohe extraheavy oils is proposed.

EXPERIMENTAL

Materials

Decane (anhydrous, 99%), tetracosane (C24, 99%), octacosane (C28, 99%), dicetyl (C32, 99%), maleic anhydride (99%), α-octadecene (90%), benzoyl peroxide (99%), *o*-xylene (98%), octadecylamine (97%), and 1-methylnaphthalene (97%) were purchased from Acros Co. and were used as obtained.

Two types of extraheavy Liaohe waxy oils from different oil wells, CO-1 and CO-2, were obtained from Petrochina Liaohe Oilfield Co. Their composition and physical properties are listed in Table I; they both contained more than 30% paraffin and 10% asphaltene, and the pour point of CO-2 was 6°C higher than that of CO-1.

According to ASTM D 3235 (Standard Test Method for Solvent Extractables in Petroleum Waxes), the wax was extracted from the crude oil. The carbon-number distribution of the paraffins extracted from the two Liaohe waxy oils was analyzed by gas chromatography–mass spectrometry (GC–MS; Figure 1).[27,28] The average carbon number of the paraffins ranging from C15 to C35 contained in the two oils (CN_{wax}) was calculated by eq. (1):[29]

$$CN_{wax} = \frac{\sum_{15}^{35}(14n+2)w_n - 2}{14}. \quad (1)$$

where n is the carbon number of each length of paraffin in crude oil and w_n is the mass fraction of each paraffin molecule in the total paraffins extracted from the Liaohe extraheavy waxy oils. The average carbon numbers of the paraffins extracted from CO-1 and CO-2 were 26 and 30, respectively.

Paraffin mixtures consisting of two types of *n*-alkane mixture was selected to mimic the paraffins in the Liaohe extraheavy oil,[23–25] where decane and methylnaphthalene were chosen as the solvent of paraffin and asphaltene, respectively (Table II). To explore the effect of MACs on the paraffin and asphaltene behavior in the Liaohe extraheavy oils, four model oils with and without asphaltenes were prepared. MO-1 and MO-2 were model oils that contained only wax, and MO-3 and MO-4 were model oils that contained both wax and asphaltenes. Before the measurements, the model oils were heated to above 60°C and stirred at this temperature for at least 30 min to remove the thermal and shearing histories.

Synthesis of the MACs

Comb-type MACs were synthesized by radical polymerization in two steps (Figure 2). In the first step, poly(maleic alkylamide-*co*-α-olefin) was synthesized by long-chain *n*-alkenes and maleic anhydride in *o*-xylene at 120°C for 1.5 h with benzoyl peroxide as an initiator under nitrogen atmosphere protection. In the second step, through amination by long-chain *n*-amines at 105–110°C for over 12 h, the MACs were synthesized. The final products were obtained by precipitation with excess methanol, filtration, washing with hot water, and vacuum drying. MACs with various ratios of polar to nonpolar groups were acquired by the variation of the feeding ratios of maleic anhydride to amine (1:1.0, 1:1.5, and 1:2.0). The corresponding copolymers were named MAC1.0, MAC1.5, and MAC2.0, respectively.

^{1}H-NMR Spectroscopy and Gel Permeation Chromatography (GPC)

^{1}H-NMR spectra were recorded on a Bruker Avance 500 spectrometer operating at 500 MHz with deuterated chloroform as a solvent. The molecular weight and molecular weight distribution of the MACs were measured by a Waters 1525 GPC instrument with tetrahydrofuran as the mobile phase and polystyrene samples as standards.

Figure 3 shows the ^{1}H-NMR spectra of the poly(maleic acid alkylamides-*co*-α-octadecene) copolymers (MAC1.0). Chemical shifts of the protons in CH_3, CH_2, and CH in the α-octadecene monomer unit appeared at 0.9, 1.2–1.8, and 2.0 ppm, respectively. Chemical shifts of the protons in the maleic acid and alkyl amide groups were found around 2.8 ppm. The integration of the protons in poly(maleic anhydride-*co*-α-octadecene)

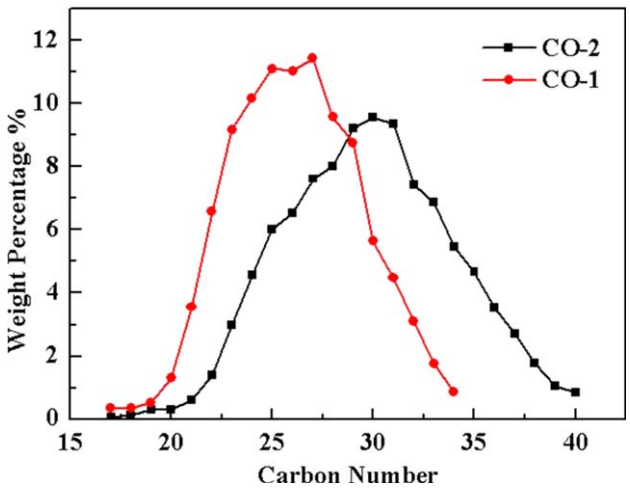

Figure 1. Carbon-number distributions of two kinds of Liaohe waxy oils analyzed with GC–MS. [Color figure can be viewed in the online issue, which is available at wileyonlinelibrary.com.]

Table II. Compositions of the Model Oils

Model oil	Decane (%)	Methylnaphthalene (%)	Asphaltene (%)	C24 (%)	C28 (%)	C32 (%)
MO-1	92	—	—	4	4	—
MO-2	92	—	—	—	4	4
MO-3	68	22	2	4	4	—
MO-4	68	22	2	—	4	4

revealed that the copolymerization ratio of maleic anhydride to α-octadecene was 1:1.09.

The amidation ratio (f) gave the number of alkyl amides formed from each maleic anhydride group of the polymer; it was between 0 and 2, as estimated from the integrated area of the peak around 0.9 ppm for the chain-terminal methyl protons (A_{CH3}) and the area of the peak around 2.8 ppm for the protons singly linked to the carbon in each maleic group (A_{CH}). For the integration of CH and CH_2 according to the relation $\frac{A_{CH}}{A_{CH_3}} = \frac{2}{3\times1.09+3f}$, f could be calculated by the equation $f = \frac{2A_{CH_3}}{3A_{CH}} - 1.09$. The calculated f values of the MACs were 0.55, 0.69, and 0.87 for MAC1.0, MAC1.5, and MAC2.0, respectively. We found that the higher the feeding ratio was, the higher f was in the copolymer.

The molecular weights of MAC1.0, MAC1.5, and MAC2.0, measured by GPC, were 12.31, 13.23, and 14.58 kg/mol, respectively.

τ_y

τ_y is defined as the stress below which no flow occurs.[13,20] An operational definition of τ_y is adopted as the stress at the transition between the creep and liquidlike viscosity regimes, where τ_y can be identified as the stress for which the derivative is a maximum. A typical unidirectional yielding test was introduced. Initially, the low applied stress was below τ_y, and the resulting viscosity was essentially infinite. As the stress increased further, the gel crept for a period of time and then catastrophically failed. So when the viscosity decreased dramatically, the corresponding stress was τ_y under the temperature.

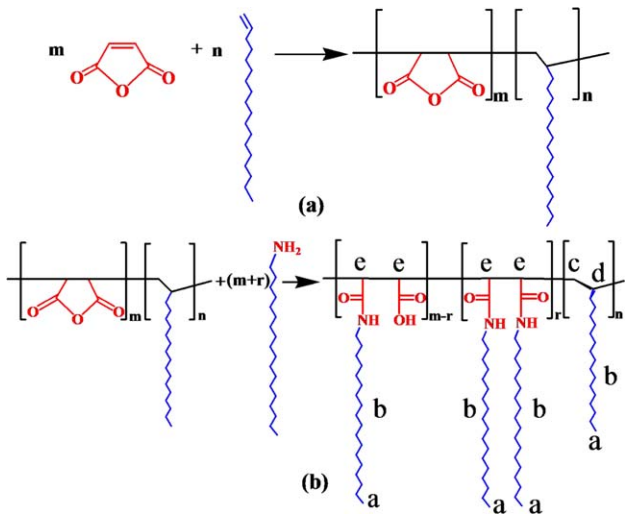

Figure 2. (a) Synthesis of poly(α-olefin-*co*-maleic anhydride amide) (MAC) and (b) MACs with different ratios of octadecylamine. [Color figure can be viewed in the online issue, which is available at wileyonlinelibrary.com.]

MACs with various f values were directly added to the crude and model oils and then heated at 80°C along with stirring for 30 min to disperse the MACs well in the oils. The measurements were performed on a MCR501 rheometer (Anton-Paar GmbH) equipped with 25-mm parallel-plate geometry. The model oil samples were initially heated to 70°C, kept at that temperature for 30 min, and then cooled to 0°C at a rate of 10°C/min for measurement. However, the Liaohe extraheavy oil samples were heated to 80°C, kept at that temperature for 30 min, and then cooled to 50°C, which was close to their WAT, at a rate of 10°C/min to determine τ_y.

Polarized Optical Microscopy

The morphology of the paraffin crystals was observed with a LEIKADM 2500P PLM with a Linkam THMS 600 cold/hot stage. Images were captured with a charge-coupled device camera connected to a PC via a WT-1000GM imaging board. A small quantity of model or waxy crude oil sample was transferred to a glass slide on the cold/hot stage for observation. Images of the model oil were taken at 0°C, and images of the waxy crude oil were taken at room temperature.

DSC

A TA2000/MDSC2910 DSC apparatus (from TA Instruments) was used to examine the crystallization of long-chain paraffin in the gels. The scanning rate was set at 10°C/min from 60 to −20°C for the model oils and from 80 to 0°C for the Liaohe extraheavy oils. All of the samples were heated to 80°C and

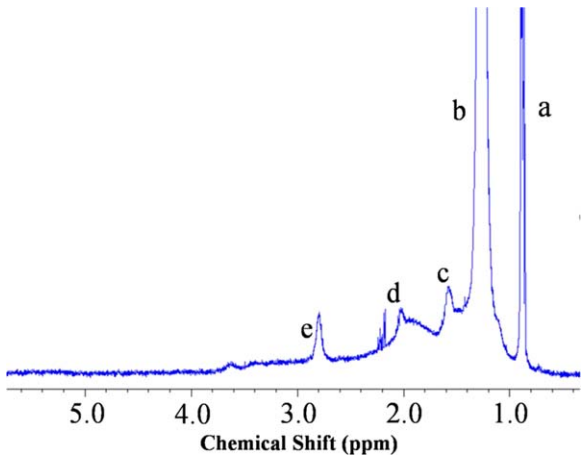

Figure 3. ^{1}H-NMR spectrum of MAC1.0. [Color figure can be viewed in the online issue, which is available at wileyonlinelibrary.com.]

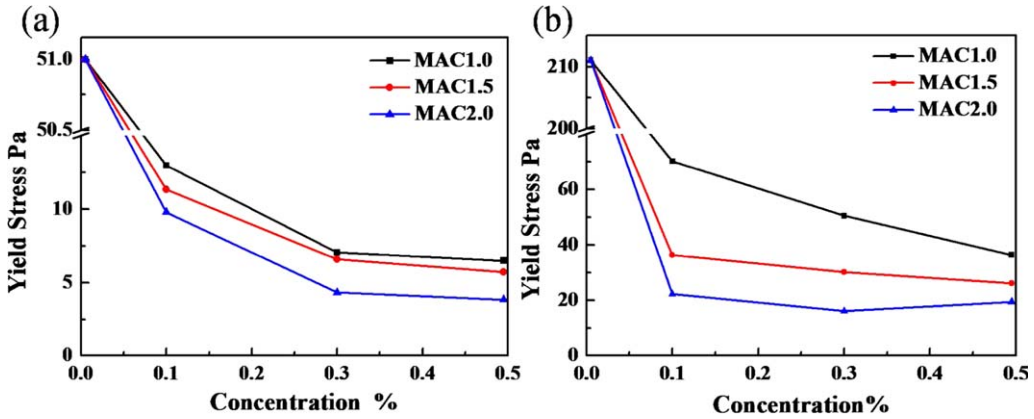

Figure 4. τ_y values of the model oils as a function of the MAC concentration: (a) MO-1 and (b) MO-2. [Color figure can be viewed in the online issue, which is available at wileyonlinelibrary.com.]

kept at this temperature for 30 min to eliminate any thermal history. The enthalpies and onset temperature (T_{onset}) of the crystallization of the paraffins were analyzed with TA Universal Analysis software.

XRD

One-dimensional images were collected in reflection mode from the dried samples of long-chain paraffin crystals with a Rigaku D/Max-2550v XRD instrument equipped with an evacuated Statton camera. X-rays with a source wavelength of 0.154 nm were produced with a sealed tube generator with a Cu target and a Huber graphite monochrometer. The scattering patterns were recorded over a range of angles corresponding to $2\theta = 5–50°$.[15]

RESULTS AND DISCUSSION

Effect of the MACs on the Model Oils

The composition of the paraffins in crude oil has an important impact on the flowability of the crude oil. On the basis of the composition of paraffins extracted from the Liaohe extraheavy

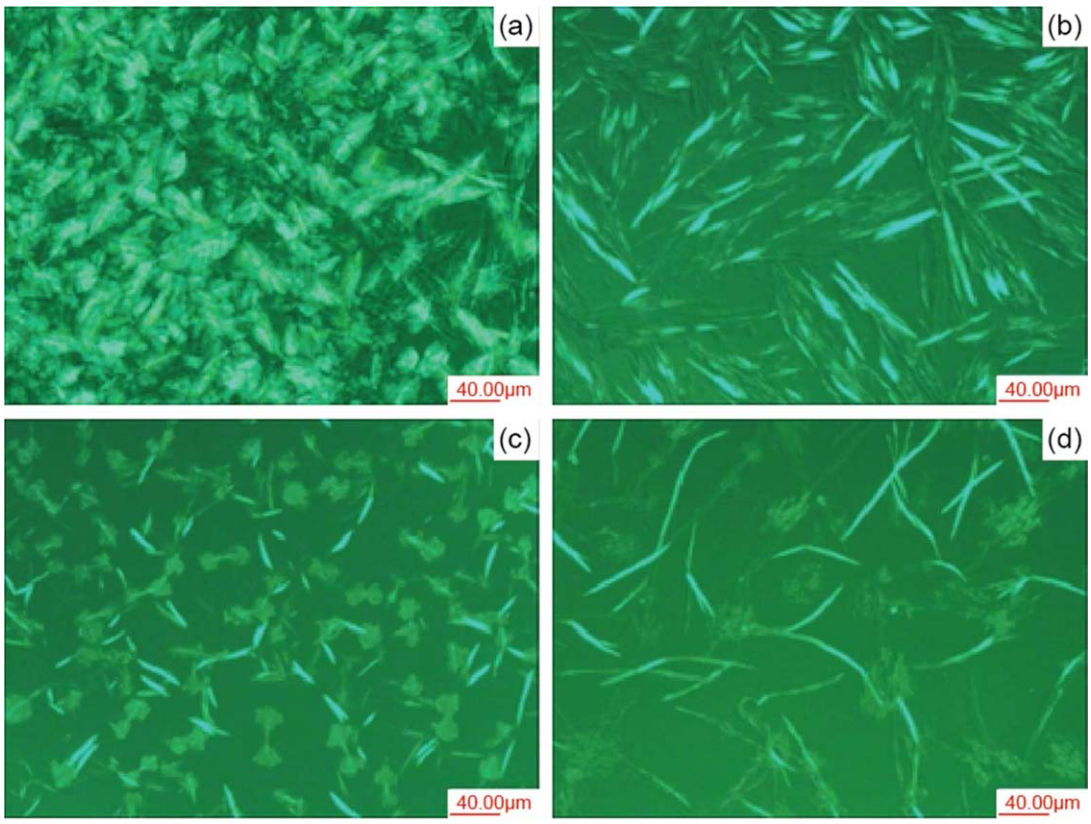

Figure 5. Polarized light micrographs of the paraffin crystals in MO-1 with and without MACs: (a) MO-1, (b) MO-1 plus 0.5 wt % MAC1.0, (c) MO-1 plus 0.5 wt % MAC1.5, and (d) MO-1 plus 0.5 wt % MAC2.0. [Color figure can be viewed in the online issue, which is available at wileyonlinelibrary.com.]

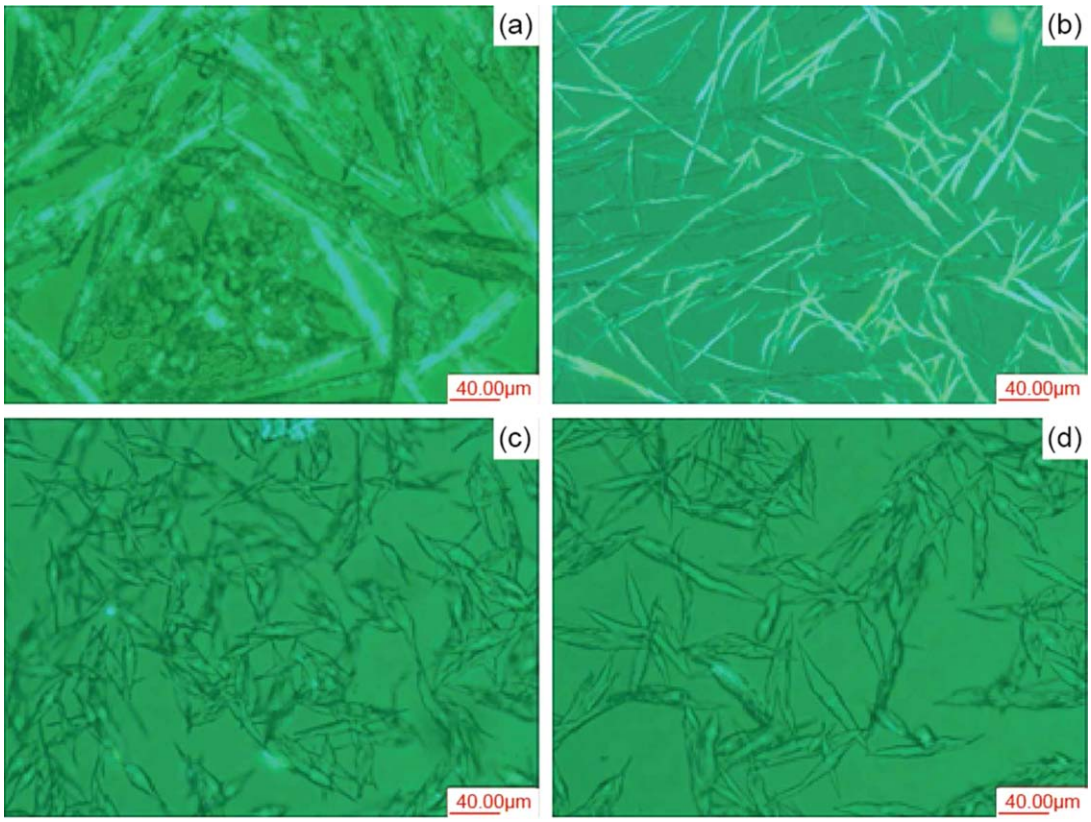

Figure 6. Morphology of paraffin crystals in MO-2 with and without MACs: (a) MO-2, (b) MO-2 plus 0.5 wt % MAC1.0, (c) MO-2 plus 0.5 wt % MAC1.5, and (d) MO-2 plus 0.5 wt % MAC2.0. [Color figure can be viewed in the online issue, which is available at wileyonlinelibrary.com.]

oils, model oils were prepared that consisted of two different paraffins with same average carbon numbers as CO-1 and CO-2, respectively.

The τ_y values upon the addition of MACs with various f values was measured by rheological methods. The MACs reduced the τ_y values of the model oils MO-1 and MO-2 without asphaltenes (Figure 4). τ_y of MO-2, with an average carbon number of 30, was higher than that of MO-1, with an average carbon number of 26. The reduction of τ_y increased with increasing f value of the MACs and the MAC concentration. The MAC with a larger f had a higher grafting density of long-chain alkyl pendants; this was beneficial for their cocrystallization with the paraffins in the model oils. Moreover, a higher concentration of MACs provided more cocrystallization opportunities with paraffins.

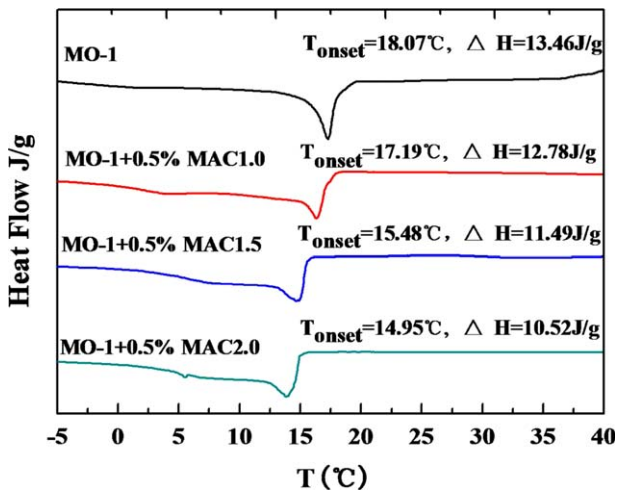

Figure 7. DSC thermograms of MO-1 with and without MACs (ΔH = enthalpies; T = temperature). [Color figure can be viewed in the online issue, which is available at wileyonlinelibrary.com.]

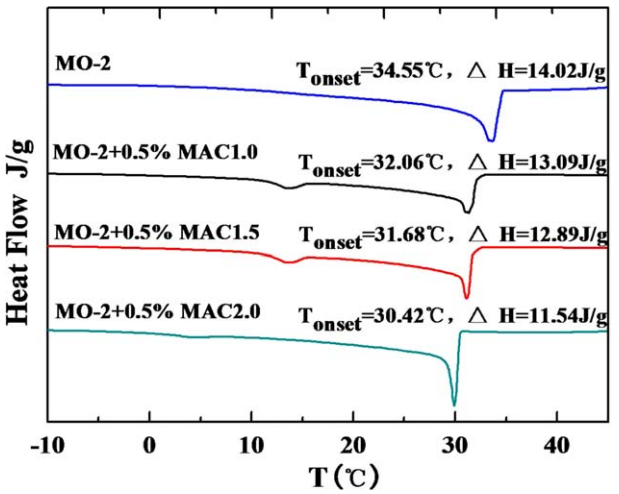

Figure 8. DSC thermograms of MO-2 with and without MACs (T = temperature). [Color figure can be viewed in the online issue, which is available at wileyonlinelibrary.com.]

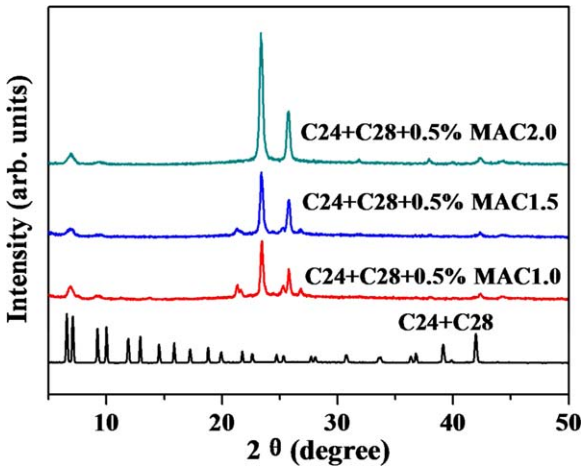

Figure 9. X-ray diffractograms of paraffin crystals from MO-1 with and without MACs. [Color figure can be viewed in the online issue, which is available at wileyonlinelibrary.com.]

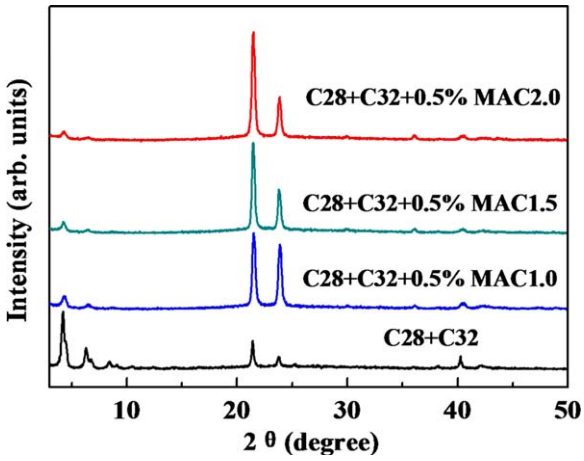

Figure 10. X-ray diffractograms of paraffin crystals from MO-2 with and without MACs. [Color figure can be viewed in the online issue, which is available at wileyonlinelibrary.com.]

The morphology of paraffin crystals from model oils was observed by polarizing light microscopy (Figures 5 and 6). After the dosage of MACs, the shape of paraffin crystals in the model oils changed from irregular to needlelike.[9] In Figure 4, the paraffin crystals in MO-1 without MACs appeared to form tightly packed leaflike particles. After the addition of MACs with a concentration of 0.5 wt %, all of the paraffin crystals in the model oils became thinner with a significantly reduced amount. Particularly for MAC2.0, the number of paraffin crystals was the lowest; this was beneficial for the improvement of the flowability of the model oils and correlated with the τ_y results.

The morphology change of the paraffin crystals in MO-2 upon the addition of the MACs was similar to that of MO-1 (Figure 6), whereas the paraffin crystals in MO-2 seemed thicker than that in MO-1; this was probably due to the higher average carbon number of the paraffins.

In a way, the crystal T_{onset} reflected the difficulty of the crystallization of paraffins in waxy oil.[30] DSC was adopted to determine T_{onset} (Figures 7 and 8). The model oils with and without the dosage of copolymers all exhibited a significant crystallization transition. T_{onset} and transition enthalpy decreased with the addition of MACs and increasing *f*. As shown in Figure 8, T_{onset} of MO-2 was much higher than that of MO-1 because of the larger average carbon number and higher crystallization potential.

XRD was used to examine the effect of the MACs on the crystal structure of paraffins separated from the model oils with and without MACs (Figures 9 and 10). For MO-1, the diffraction peaks belonging to C24 were isolated with those belonging to C28, which implied that C24 and C28 could not cocrystallize well with each other. The addition of the MACs totally changed the crystal patterns of C24 and C28 (Figure 9). The MACs greatly reduced the low-angle diffractions peaks and increased the middle-angle diffractions around 20–30°, which are typical diffractions of monoclinic paraffin crystals. The amorphous portion of the copolymers disturbed the stacking of the paraffin crystal platelets. A reasonable explanation may be that the MACs inhibited the formation and growth of large crystals from either C24 or C28.

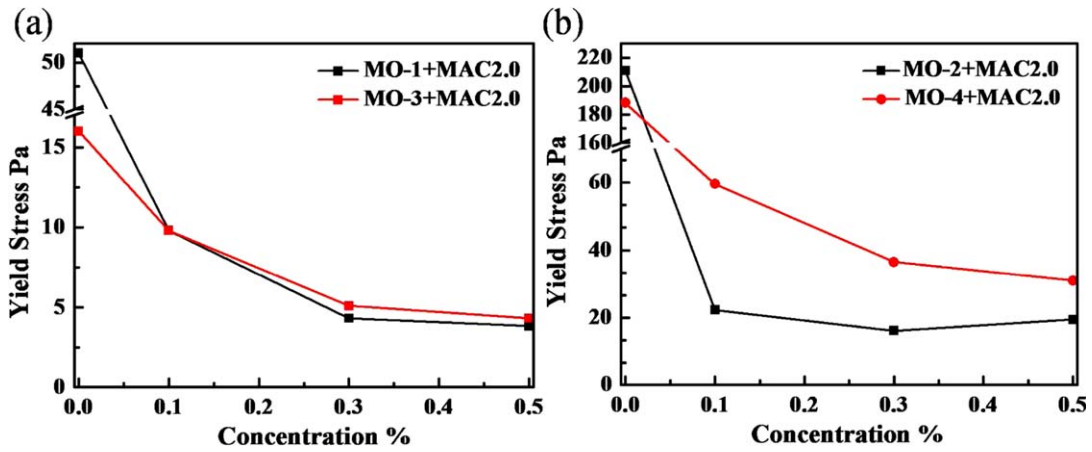

Figure 11. τ_y values of the model oils with and without asphaltenes as a function of the MAC2.0 concentration: (a) MO-1 and MO-3 and (b) MO-2 and MO-4. [Color figure can be viewed in the online issue, which is available at wileyonlinelibrary.com.]

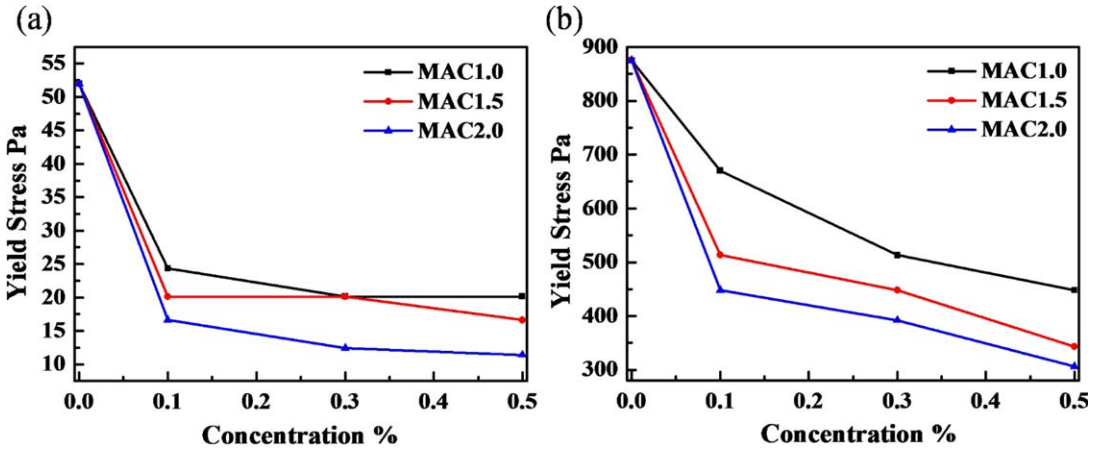

Figure 12. τ_y values of the Liaohe extraheavy oils as a function of the MAC concentration: (a) CO-1 and (b) CO-2. [Color figure can be viewed in the online issue, which is available at wileyonlinelibrary.com.]

Unlike MO-1, MO-2 in the absence of MACs showed a good eutectic of C28 and C32 (Figure 10). However, in the presence of MACs, similar trends were found in that the packing structure was weakened and monoclinic paraffin crystals were enhanced, especially with the increase of f of the MACs. This correlated with the results of DSC.

To explore the effect of asphaltenes, asphaltenes extracted from the Liaohe extraheavy oils were added to the model oils (Table II). Interestingly, the τ_y values of the model oils with asphaltenes (MO-3 and MO-4) were lower than those without asphaltenes (MO-1 and MO-2); this was probably because of the effect of the asphaltenes as natural pour-point depressants (Figure 11).[9,23] Upon the addition of the MACs, all of the τ_y values were reduced, whereas the efficiency in the reduction of τ_y weakened in the presence of asphaltenes.

MACs were designed to both control the paraffin crystallization and disperse the asphaltenes in traditional crude oils. Without asphaltenes, the MACs fully participated in the cocrystallization

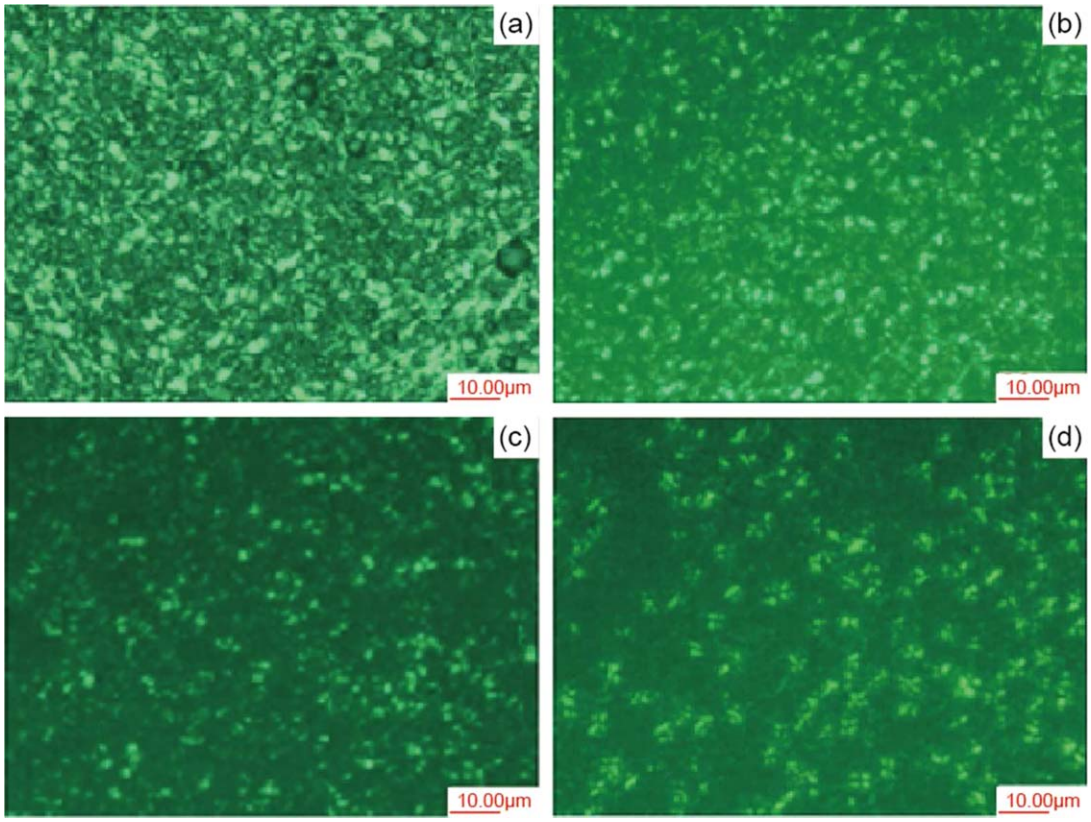

Figure 13. Polarizing light micrographs of CO-1 with and without MACs: (a) CO-1, (b) CO-1 plus 0.5 wt % MAC1.0, (c) CO-1 plus 0.5 wt % MAC1.5, and (d) CO-1 plus 0.5 wt % MAC2.0. [Color figure can be viewed in the online issue, which is available at wileyonlinelibrary.com.]

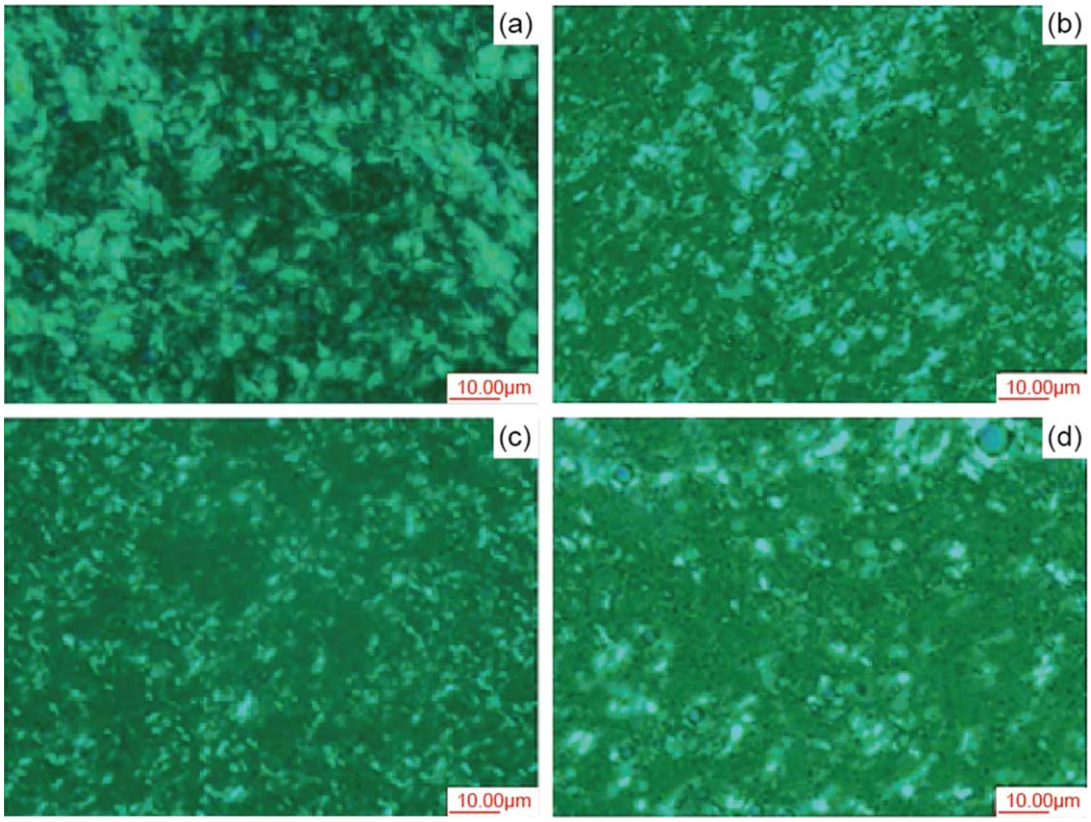

Figure 14. Polarizing light micrographs of CO-2 with the dosage of MACs: (a) CO-2, (b) CO-2 plus 0.5 wt % MAC1.0, (c) CO-2 plus 0.5 wt % MAC1.5, and (d) CO-2 plus 0.5 wt % MAC2.0. [Color figure can be viewed in the online issue, which is available at wileyonlinelibrary.com.]

with paraffins in the model oils (MO-1 and MO-2), whereas part of them were used to disperse asphaltenes in the model oils with asphaltenes (MO-3 and MO-4).

Effect of the MACs on the Liaohe Extraheavy Oils

As shown in Figure 12, the τ_y values of the Liaohe extraheavy oils CO-1 and CO-2 were all reduced significantly by 0.1 wt % MACs, whereas further addition showed a decreased effect for CO-2 and no impact for CO-1. It seemed that MACs with higher f values showed slightly better results on reducing the yield.

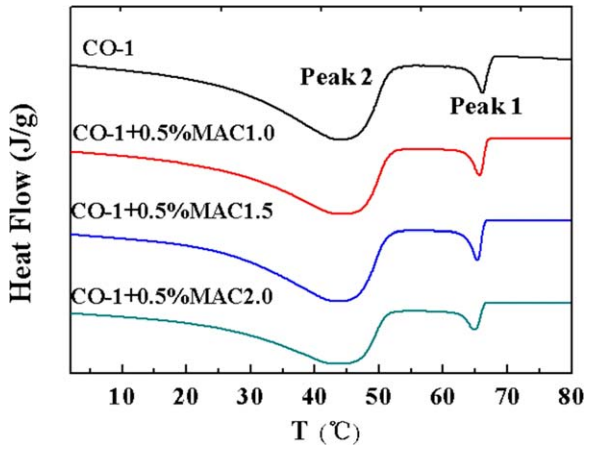

Figure 15. DSC thermographs of CO-1 with and without the dosage of MACs during cooling at a rate of 10°C/min (T = temperature). [Color figure can be viewed in the online issue, which is available at wileyonlinelibrary.com.]

The morphology of the paraffin crystals in the Liaohe waxy oils was observed by polarizing light microscopy (Figure 13). Many crystals from CO-1 without MACs appeared and were packed tightly. Upon the addition of the MACs, both the amount and size of the paraffin crystals decreased. Among the three MACs, MAC2.0 resulted in the smallest number of paraffin crystals, and this was correlated to the τ_y measurements of CO-1.

The morphologies of CO-2 with and without MACs are shown in Figure 14. Similarly, the MACs effectively hindered the

Table III. Thermal Data for CO-1 during Cooling

	Peak 1		Peak 2		
Sample	Peak (°C)	T_{onset}	Peak (°C)	T_{onset}	ΔH_{Total} (J/g)
CO-1	66.2	67.5	44.1	51.6	92.7
CO-1 plus 0.5% MAC1.0	65.7	66.8	44.0	51.5	86.7
CO-1 plus 0.5% MAC1.5	65.4	66.4	43.9	51.2	86.1
CO-1 plus 0.5% MAC2.0	65.0	66.3	43.8	51.0	67.0

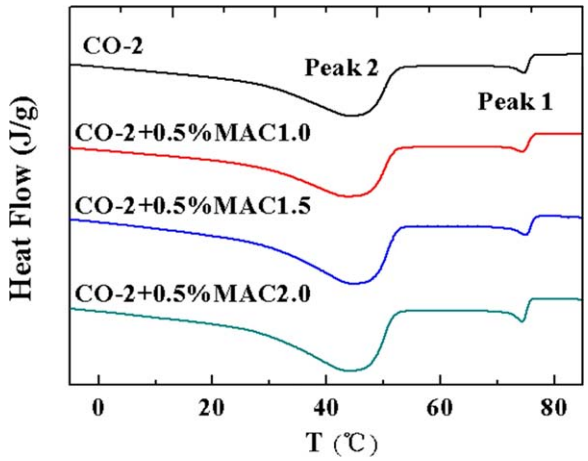

Figure 16. DSC thermographs of CO-2 with and without the dosage of MACs at a rate of 10°C/min during cooling (T = temperature). [Color figure can be viewed in the online issue, which is available at wileyonlinelibrary.com.]

appearance of paraffin crystals and decreased the crystal size. Moreover, the crystal size of paraffin in CO-2 seemed larger than that in CO-1; this was probably due to the larger average carbon number of the paraffins.

The DSC results of CO-1 with the addition of 0.5 wt % MACs are shown in Figure 15. In the thermogram, all of the cooling curves had two distinct transitions, which corresponded to the two crystallization behaviors in CO-1. The thermal data from the DSC thermograph of CO-1 are collected in Table III; these include the T_{onset} values of the two peaks and the total enthalpy of transition (ΔH_{Total}). The MACs reduced the T_{onset} and peak temperature values of both the paraffin crystallization peaks and ΔH_{Total}'s in CO-1. When the f values of the MACs increased, the T_{onset} and ΔH_{Total} decreased monotonically.

Figure 16 shows the DSC curves of CO-2 with and without MACs upon cooling, and corresponding thermal data are listed in Table IV. Compared to the thermal data of CO-1, CO-2 showed similar changes with the addition of the MACs. The MACs decreased T_{onset} and the peak temperature of both paraffin crystallization peaks and ΔH_{Total}, whereas the T_{onset} and ΔH_{Total}'s in CO-2 were higher; this coincided with the fact that

Table IV. Thermal Data for CO-2 during Cooling

	Peak 1		Peak 2		
Sample	Peak (°C)	T_{onset} (°C)	Peak (°C)	T_{onset} (°C)	ΔH_{Total} (J/g)
CO-2	74.9	76.2	43.9	52.0	106.1
CO-2 plus 0.5% MAC1.0	74.7	76.0	43.8	51.8	104.4
CO-2 plus 0.5% MAC1.5	74.5	75.9	43.4	51.8	99.8
CO-2 plus 0.5% MAC2.0	74.5	75.7	43.7	51.7	99.8

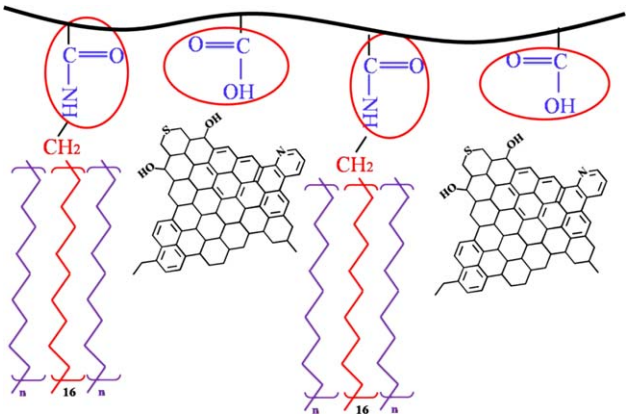

Figure 17. Assembly model of MACs with paraffins and asphaltenes for the improvement of the cold flowability of the Liaohe waxy oil. [Color figure can be viewed in the online issue, which is available at wileyonlinelibrary.com.]

the average carbon number of the paraffins in CO-2 (30) was higher than that of CO-1 (26).

On the basis of the experimental results, the assembly of comb-type MACs with the paraffins and asphaltenes in the Liaohe extraheavy oils is proposed and is shown in Figure 17. The nonpolar alkyl pendants of the MACs could cocrystallize with long-chain paraffins, whereas the polar groups covered the crystal surfaces and hindered the growth of crystals; this was indicated by the reduction of τ_y, the smaller size of the paraffin crystals, and the lower T_{onset} and ΔH_{Total}.[13,15,22] MACs with higher f values had more alkyl side chains; this should have made them more effective for cocrystallizing with paraffins. The polar groups in the MACs could disperse the asphaltenes and prevent them from aggregating (Figure 17). In this way, the flowability of the Liaohe extraheavy oils could be improved.

The information on how the MACs improved the flowability of the Liaohe extraheavy oils could endow comb-type MACs with great potential for the enhancement of the production of heavy oils with extremely high contents of paraffins and asphaltenes.

CONCLUSIONS

Liaohe extraheavy oils with high contents of both paraffins and asphaltenes are solid up to 60°C. To improve their flowability, a comb-type poly(maleic alkylamide-*co*-α-octadecene) amidated by octadecylamine (MACs) with various f values were synthesized. Model oils of paraffin mixtures, which had the same average carbon number as the paraffins extracted from Liaohe extraheavy oils, with and without asphaltenes were used to explore the effect of MACs on the control of the paraffin crystallization and asphaltene dispersion. We found that MACs reduced τ_y, decreased the paraffin crystal size, suppressed the formation of crystal platelets, delayed the crystallization of paraffins, and hindered the growth of paraffin crystals from the model oils, as revealed by rheology, PLM, DSC, and XRD. The same effects of the MACs on the τ_y, morphology, and crystallization behaviors of paraffins in the Liaohe extraheavy oils were also observed. The MAC with the higher f and higher concentration seemed more effective in controlling the crystallization

of the paraffins. They seemed to be suitable for improving the flowability of the Liaohe extraheavy oils.

ACKNOWLEDGMENTS

Financial support from the National Natural Science Foundation of China (contract grant numbers 51003028, 21004021, and 11076001/A06) and Fundamental Research Funds for the Central Universities is gratefully acknowledged. The authors also thank Petrochina Liaohe Oilfield Co. for oil samples and technological support.

REFERENCES

1. Venkatesan, R.; Ostlund, J. A.; Chawla, H.; Wattana, P.; Nyden, M.; Fogler, H. S. *Energy Fuels* **2003**, *17*, 1630.
2. Singh, P.; Venkatesan, R.; Fogler, H. S.; Nagarajan, N. R. *AIChE J.* **2001**, *47*, 6.
3. El-Gamal, I. M.; Atta, A. M.; Al-Sabbagh, A. M. *Fuel* **1997**, *76*, 1471.
4. Balabin, R. M.; Syunyaev, R. Z.; Schmid, T.; Stadler, J.; Ekaterina, I. L.; Zenobi, R. *Energy Fuels* **2011**, *25*, 189.
5. Likhatskya, V. V.; Balabinb, R. M.; Syunyaeva, R. Z. *J. Dispersion Sci. Technol.* **2011**, *32*, 1502.
6. Balabin, R. M.; Syunyaev, R. Z. *J. Colloid Interface Sci.* **2008**, *318*, 167.
7. Syunyaeva, R. Z.; Balabinb, R. M. *J. Dispersion Sci. Technol.* **2008**, *29*, 1505.
8. Syunyaeva, R. Z.; Balabinb, R. M.; Akhatov, I. S. *Energy Fuels* **2009**, *23*, 1230.
9. Xu, J.; Qian, H.; Xing, S.; Li, L.; Guo, X. *Energy Fuels* **2011**, *25*, 573.
10. Gilby, G. W. *Spec. Publ. RSC* **1983**, *45*, 108.
11. Ashbaugh, H. S.; Guo, X.; Schwahn, D.; Prud'homme, R. K.; Richter, D.; Fetters, L. *J. Energy Fuels* **2005**, *19*, 138.
12. Ashbaugh, H. S.; Fetters, L. J.; Adamson, D. H.; Prud'homme, R. K. *J. Rheol.* **2002**, *46*, 763.
13. Guo, X.; Pethica, B. A.; Huang, J. S.; Prud'homme, R. K.; Adamson, D. H.; Fetters, L. *J. Energy Fuels* **2004**, *18*, 930.
14. Guo, X.; Pethica, B. A.; Huang, J. S.; Prud'homme, R. K. *Macromolecules* **2004**, *37*, 5638.
15. Li, L.; Guo, X.; Adamson, D. H.; Pethica, B. A.; Huang, J. S.; Prud'homme, R. K. *Ind. Eng. Chem. Res.* **2011**, *50*, 316.
16. Garcia, M. C. *Energy Fuels* **2000**, *14*, 1043.
17. Fang, L.; Zhang, X. D.; Ma, J. H.; Zhang, B. T. *Ind. Eng. Chem. Res.* **2012**, *51*, 11605.
18. Castro, L. V.; Flores, E. A.; Vazquez, F. *Energy Fuels* **2011**, *25*, 539.
19. Wu, Y. M.; Ni, G. D.; Yang, F.; Li, C. X.; Dong, D. G. *Energy Fuels* **2012**, *26*, 995.
20. Xu, J.; Xing, S.; Qian, H.; Chen, S.; Wei, X.; Zhang, R.; Li, L.; Guo, X. *Fuel* **2013**, *103*, 600.
21. Xu, J.; Zhang, X.; Sun, J.; Li, L.; Guo, X. *Asia-Pac. J. Chem. Eng.* **2009**, *4*, 551.
22. Li, L.; Xu, J.; Tinsley, J.; Adamson, D. H.; Pethica, B. A.; Huang, J. S.; Prud'homme, R. K.; Guo, X. *AIChE J.* **2012**, *58*, 2254.
23. Tinsley, J.; Prud'homme, R. K.; Guo, X.; Adamson, D. H.; Callahan, S.; Amin, D.; Shao, S.; Kriegel, R. M.; Saini, R. *Energy Fuels* **2007**, *21*, 1301.
24. Tinsley, J.; Jahnke, J.; Dettman, H. D.; Prud'homme, R. K. *Energy Fuels* **2009**, *23*, 2056.
25. Garcia, M. C.; Carbognani, L.; Orea, M.; Urbina, A. *J. Pet. Sci. Eng.* **2000**, *25*, 99.
26. Borthakur, A.; Chanda, D.; Choudhury, S. R.; Rao, K. V.; Subrahmanyam, B. *Energy Fuels* **1996**, *10*, 844.
27. Espada, J. J.; Coutinho, J. A. P.; Pena, J. L. *Energy Fuels* **2010**, *24*, 1837.
28. Nguyen, X. T.; Hsieh, M.; Philp, R. P. *Org. Geochem.* **1999**, *30*, 119.
29. Yi, S.; Zhang, J. *Energy Fuels* **2011**, *25*, 1686.
30. Machado, A. L. C.; Lucas, E. F.; Gonzalez, G. *J. Pet. Sci. Eng.* **2001**, *32*, 159.